

1 **Measurement report:**

2 **Intra-annual Variability of Black/Brown Carbon and Its Interrelation with**
3 **Meteorological Conditions over Gangtok, Sikkim**

4 Pramod Kumar¹, Khushboo Sharma¹, Ankita Malu², Rajeev Rajak², Aparna Gupta¹,
5 Bidyutjyoti Baruah¹, Shailesh Yadav¹, Thupstan Angchuk¹, Jayant Sharma¹, Rakesh Kumar
6 Ranjan^{1#}, Anil Kumar Misra¹, and Nishchal Wanjari¹

7 ¹DST's Centre of excellence on Water Resources, Cryosphere and Climate Change Studies,
8 Department of Geology, Sikkim University, Gangtok, Sikkim, India -737102

9 ²Department of Geology, Sikkim University, Gangtok, Sikkim, India -737102

10 [#]Corresponding Author: rkranjan@cus.ac.in

11
12 **Abstract**

13 Black carbon (BC) and brown carbon (BrC) have versatile nature_s, and they have an apparent
14 role in ~~the~~ climate variability and changes. As the anthropogenic activity is surging, the BC
15 and BrC are also reportedly increasing. So, the monitoring of BC/BrC and observation of land
16 use land cover changes (LULCC) at a regional level are necessary for the various
17 interconnected meteorological phenomena_l changes. The current study investigates BC, BrC,
18 CO₂, BC from fossil fuels (BC_{ff}), BC from biomass burning (BC_{bb}), LULCC, and their
19 relationship to the corresponding meteorological conditions over Gangtok in the Sikkim
20 Himalayan region. The concentration of BC (BrC) 43.5 µg/m³ (32.0 µg/m³) ~~is-was~~ found to be
21 highest during the March-2022 (April-2021). Surface pressure exhibits a significant positive
22 correlation with BC, BC_{ff}, BC_{bb}, and BrC. Higher surface pressure results in a calmer and more
23 stable boundary layer, which effectively retains accumulated contaminants. Conversely, the
24 wind appears to facilitate the dispersion of pollutants, showing a strong negative
25 correlation. Surface pressure has been found to have a significant positive correlation with BC,
26 BC_{ff}, BC_{bb} and BrC. The boundary layer is calmer and more stable when the surface pressure
27 is higher, which keeps contaminants deposited there. The wind, on the other hand, appears to
28 represent the dispersion of pollutants with a strong negative correlation. The fact that all
29 pollutants and precipitation have been shown to behave similarly points to moist scavenging
30 of the pollutants. Despite the dense cloud cover, it is clear that the area is not receiving
31 convective precipitation, implying that orographic precipitation is occurring over the region.
32 Most of Sikkim receives convective rain from May to September, indicating that the region
33 has significant convective activity contributed from the Bay of Bengal during the monsoon
34 season. Furthermore, monsoon months have the lowest concentrations of BC, BC_{bb}, BC_{ff}, and

Formatted: Subscript

Formatted: Subscript

Formatted: Subscript

Formatted: Subscript

Formatted: Subscript

Formatted: Subscript

35 BrC, suggesting the potential of convective rain (as rain out scavenging) to remove most of
36 the pollutants. Moreover, BC and BrC show positive radiative feedback.

37 **Key-words:** Black carbon; Brown carbon; LULC; Sikkim Himalaya; Meteorology; Biomass
38 burning; Radiative forcing.

39 **1.0 Introduction**

40 Black carbon (BC), and brown carbon (BrC), are part of fine particulates in air pollution that
41 have a apparentdeceptive role in the climate variability and changes. BC/BrC is a short-lived
42 climate pollutant with a lifetime of only days to weeks after release in the atmosphere
43 (Pierrehumbert, 2014). During this short period of time, BC/BrC can have significant direct
44 and indirect impacts on the climate, cryosphere, agriculture, and human health (Shindell et al.,
45 2012). It consists of pure carbon in several interconnected forms. BC is formed through the
46 incomplete combustion of fossil fuels, biofuel, and biomass, and is one of the main types of
47 particles in both anthropogenic and naturally occurring soot (Bond et al., 2004). BrC in the
48 atmosphere have has been attributed to the burning of biomass and fossil fuels, the biogenic
49 release of fungi, plant debris, and humic matter, and multiphase reactions between the gas-
50 phase, particulate, and cloud microdroplet constituents in the atmosphere (Laskin et al., 2015).
51 BC/BrC is transported from its source to many locations across the world (Ramanathan and
52 Carmichael, 2008). The BC/BrC released into the atmosphere exhibits vertical distribution and
53 follows the prevailing wind speed and direction. It engages with various atmospheric
54 components before eventually settling on the Earth's surface through either wet or dry
55 deposition processes. Its hygroscopic properties render it more prone to cloud seeding and
56 cloud formation, thereby contributing directly to the precipitation mechanism in regions with
57 high humidity~~The released BC/BrC is vertically distributed and travels through the atmosphere~~
58 ~~according to wind speed and direction, interacting with numerous components before sinking~~
59 ~~on the earth's surface through wet or dry deposition. Its hygroscopic nature makes more~~
60 ~~susceptible to cloud seeding and cloud formation process and so directly helps in precipitation~~
61 ~~mechanism in high humid conditions~~ (Stevens and Feingold, 2009). In addition, it absorbs both
62 incoming and outgoing radiation, atmospheric BC/BrC modifies radiative forcing, disturbs
63 atmospheric stability, regional circulation, and rainfall pattern, affects cloud albedo, material
64 damage, reduces agricultural productivity, degrades ecosystem, and affects human health
65 (Zhang et al., 2013). However, due to an insufficiency of observations, BrC is one of the least
66 understood and uncertain warming agents (Yue et al., 2022). Numerous studies have been
67 conducted to analyze the global distribution of BC and BrC, including research focused on
68 these species within India as well ~~Several studies have been carried out to examine the~~
69 ~~concentration of BC and BrC all over the world and in India as well~~ (Reddy and Venkataraman,
70 2002a, 2002b; Venkataraman et al., 2006; Park et al., 2010; Sloss, 2012; Helin et al., 2021;
71 2020; Kumar et al., 2020a; Watham et al., 2021; Bhat et al., 2022; Runa et al., 2022; Yue et
72 al., 2022; Kumar et al, 2018b). However, the overall worldwide BC emission is estimated to

73 be 4800-7200 Gg per year (Klimont et al., 2017). In 2001, India's total BC emissions were
74 projected to be 1343.78 Gg (Sloss, 2012). Residential fuel burning and transportation
75 contribute maximum to the global anthropogenic BC emission (Helin et al., 2021). About 60
76 to 80% of residential fuels (coal and biomass) emissions are reported from Asian and African
77 countries, whereas approximately 70% of diesel engine ~~emission emissions is~~ are found to be
78 from Europe, North America, and Latin America (Johnson et al., 2019; Ayompe et al., 2021;
79 Adeeyo et al., 2022; Sun et al., 2022).

80 On the other hand, emissions on the Indian subcontinent have increased by 40% since the year
81 ~~of~~ 2000 (Kurokawa and Ohara, 2020; Sun et al., 2022). According to Reddy and Venkataraman
82 (2002a, 2002b), the estimated BC emissions in India are fossil fuels, 100 Gg biofuel, 207 Gg
83 open burning, and 39 Gg with a climatic forcing of +1.1 W/m², black carbon is the second-
84 most significant human emission in the current atmosphere (Sharma et al., 2022). BC
85 concentration was measured by Zhao et al. (2017) in the south-eastern Tibetan Plateau (TP).
86 Daily mean BC loadings ranged from 57.7 to 5368.9 ng/m³ demonstrating a high BC burden
87 even at free tropospheric altitudes (Zhao et al., 2017). Black carbon (BC) deposition was
88 estimated at the Nepal Climate Observatory - Pyramid (NCO-P) site in the Himalayan region
89 during the pre-monsoon season (March-May). A total BC deposition rate of 2.89 µg/m³/day
90 was estimated, resulting in a total deposition of 266 µg/m³ for March–May (Yasunari et al.,
91 2010). From the Indian perspective, several key short-term incidents contribute to a rise in
92 India's BC concentration from biomass burning and other sources (Kumar et al., 2020a).
93 Burning agricultural waste (stubble) is widespread in India and several other nations. Many
94 studies suggest ~~that~~ increased BC in northern India, notably ~~the Indo-Gangetic plain~~ Plain
95 (IGP) is the global absorbing aerosol hotspot (Venkataraman et al., 2006; Ramanathan and
96 Carmichael, 2008). In India, post-monsoon paddy crop waste burning occurs in the months ~~of~~
97 October and November in ~~the~~ north and northwest parts of India (Venkataraman et al., 2006).
98 In the north-western Indo-Gangetic Plain (IGP) (especially- Punjab, Haryana, and western
99 Uttar Pradesh), stubble burning is a popular practice (Venkataraman et al., 2006). Long-
100 distance transport of BC aerosols, mostly from Asia to the ~~north~~ North Pacific and South
101 America to the southwest Atlantic, is often ~~recognised~~ recognized as a significant factor in
102 local concentration (Evangelista et al., 2007). However, in India, only local sources (89%)
103 affects BC concentrations (Zhang et al., 2013), as there aren't many movements of
104 transboundary aerosols contribution over the IGP (Kumar et al., 2018a; Kedia et al., 2014;
105 Ramachandran and Rupakheti, 2022; Ramachandran et al., 2020). Both marine and continental

106 air masses contributed to total aerosol loading over middle-IGP (Kumar et al., 2017; Shukla et
107 al., 2022).

108 Black carbon is a light-absorbing particle that ~~are-is~~ released into the atmosphere directly in
109 the form of ultrafine (<0.1 µm) to fine particles (<2.5µm) (Gupta et al., 2017). BC is a good
110 tracer for particle deposition as it is non-volatile, insoluble, and chemically inert, and it can
111 also mix well with other aerosol species in the atmosphere (Kiran et al., 2018). As a result, BC
112 deposition data are important not just for BC sinks but also for a broader understanding of
113 aerosol deposition. BC emissions are mostly influenced by significant changes in the energy
114 sector, fuel usage, industrial expansion, and an increase in the number of vehicles (Bisht et al.,
115 2015). Residential ~~fuels~~ like wood, agricultural waste, and cow dung used for cooking and
116 biomass usage for home purposes are the primary sources of BC emissions (Venkataraman et
117 al., 2006). The Asian mainland is a substantial contributor to global BC emissions and has
118 been identified as a hotspot (Gupta et al., 2017). BC has a high absorption ability, accounting
119 for 90-95 percent of total atmospheric aerosol absorption (Hansen et al., 1984). It can absorb
120 solar energy in the visible-infrared band and warm the environment. In comparison to carbon
121 dioxide, BC has a much shorter life cycle in the atmosphere. As a result, mitigation or reduction
122 has a greater positive impact on the atmosphere (Kirchstetter et al., 2004; Takemura and
123 Suzuki, 2019). Changing land use land cover (LULC) has a very significant impact on weather,
124 climate, and aerosols (Mahmood et al., 2010). It is well well-stabilised fact that the LULC
125 change has a direct relation with land surface temperature, vehicular emission, and
126 anthropogenic activity (Aithal and MC, 2019). ~~Which This~~ motivated the present study for ~~the~~
127 further analysis ~~for-of~~ Sikkim region land use land cover change and its relation with
128 temperature and BC/BrC for ~~the~~ March 2021 to March 2022. The current study's objectives
129 are to assess the intra-annual variability of Black/Brown Carbon (BC/BrC)
130 (diurnal/daily/monthly) during the study period March-2021 to March-2022, as well as the
131 interrelationship between meteorological conditions and BC/BrC, along with LULC change
132 for three decades 2000, 2010, and 2020, and its relationship with anthropogenic activity over
133 Gangtok.

134 2.0 Study location

135 The Gangtok Municipal Corporation (GMC) has been selected for the present study on the
136 basis of its urban ~~exposer-exposure~~ and settlement change for three decades as well as
137 congruently temperature rise (Figure S1). The sampling ~~has been was~~ carried out at the Pani
138 House area in Gangtok, GMC, having a longitude of 88.609°E and a latitude of 27.323°N.

139 Sikkim is surrounded by Nepal, China, and Bhutan from west, north, and east respectively,
140 and consists of the trans and greater Himalayan range. Moreover, Sikkim has one of the most
141 fragile forest covers. However, Gangtok is a densely populated city and capital of the state
142 of Sikkim which is situated in the East Sikkim district (see Figure 1a). The population
143 of Sikkim has been found to have increased as per the Indian census for three decades
144 as this can be seen in table S1.

145 3.0 Data and Methodology

146 The real-time sampling of BC was carried out from 10th March 2021 to 17th March 2022,
147 at Gangtok using the seven-channels dual spot Aethalometer (Model AE-33-7, Magee
148 Scientific, USA). The data was collected for the measurement of BC and BrC associated with
149 particulate matter having an aerodynamic diameter of less than 2.5 μm (PM_{2.5}). The
150 concentration of BC, BrC, BC_{bb}, and BC_{ff} have been estimated by the Carbonaceous Aerosol
151 Analysis Tools (CAAT) software tool from the Magee Scientific Aethalometer model AE33
152 (Hansen and Schnell, 2005). The carbon dioxide (CO₂) was measured using a CO₂ sensor
153 (Vaisala-GMP343) which is attached to the aethalometer. The inlet of the aethalometer was
154 mounted at a height of 15 m above ground level. One of the main sources of uncertainty in
155 using aerosol absorption measurements to estimate the BrC absorption coefficient at 370 nm
156 BrC mass concentration is the fact that other species, such as black carbon and dust, can also
157 contribute to the measured absorption. This can lead to overestimation of BrC mass
158 concentration, particularly in environments where these species are also present. However, the
159 Sikkim region has one of the higher precipitation regions in the world and
160 negligible contribution of dust pollution. Furthermore, there must be lesser over/under
161 estimation. Therefore, the present study used mass concentration.

162 A new data set of BC, BrC, Black Carbon from biomass burning (BC_{bb}), Black Carbon from
163 fossil fuels (BC_{ff}), the BrC, percentage contribution of biomass burning to BC (BB%) and CO₂
164 has been generated over the unreported region of Sikkim Himalaya. The diurnal and monthly
165 data sets of BC, BC_{bb}, BC_{ff}, BrC, BB%, and CO₂ have been given in the details in
166 supplementary materials (Table S2 and S3). In addition to this, the meteorological data has
167 been selected for ERA5 reanalysis for the study. LULC data has been taken from USGS earth
168 explorer of 2000 and 2010 Landsat-5, 2020 Landsat-8, and 2021 for Sentinel-
169 2 (Karra et al., 2021). LULC data has been chosen for the month of December to minimize the
170 cloud cover. The details of the LULC calculation steps used are given in the supplementary
171 section (methodology S1.3). The brief of the data set is discussed in the table 1.

Formatted: Subscript

Formatted: Subscript

Formatted: Subscript

Formatted: Subscript

Formatted: Subscript

Formatted: Subscript

172 **3.1 Estimation of BrC**

173 The Carbonaceous Aerosol Analysis Tools (CAAT) software tool from the Magee Scientific
 174 Aethalometer model AE33 was utilized to estimate the concentrations of BC, BrC, BC_{bb}, and
 175 BC_{fr}. The absorption coefficients of BC and BrC were determined using the multi-wavelength
 176 absorption coefficients provided by the aethalometer. The presence of BrC was identified by
 177 observing the maximum light absorption between 370–590 nm, but its absorption may increase
 178 significantly below this range depending on its composition. The attenuation of illumination
 179 measured in this study using the aethalometer was attributed solely to the contribution of BC
 180 and BrC. It is believed that the absorption coefficient at 370 nm measured by the aethalometer
 181 represents the combined absorption coefficients of BC and BrC, which is denoted as $\sigma_{BC + BrC}$
 182 (370 nm). This assumption is similar to the model used in the multi-wavelength absorbance
 183 analyzer (MWAA) approach for source allocation, as described in Massabò et al. (2015).
 184 Equation (13-13) was used to calculate the σ_{BrC} (370 nm) absorption coefficient
 185 (supplementary methodology S1), which involved subtracting the contribution of BC (σ_{BC} (370
 186 nm)) from the observed absorption coefficient ($\sigma_{BC + BrC}$ (370 nm)).

187
$$\sigma_{BrC}(370 \text{ nm}) = \sigma_{BC + BrC}(370 \text{ nm}) - \sigma_{BC}(370 \text{ nm})$$

 188 _____ Eq. (1)

189 The σ_{BC} (370 nm), was calculated by applying the power-law fit to absorption data in the 590-
 190 950 nm wavelength range provided in equation (1).

191
$$\sigma_{BC}(\lambda) = \beta \lambda^{-AAE_{BC}}$$
 Eq.
 192 (2)

193 The absorption angstrom exponent of BC is denoted as AAE_{BC}, with β being a constant value.
 194 As BC is a significant contributor to light absorption at wavelengths beyond 590 nm, the
 195 contribution of other aerosol species can be neglected, and the AAE_{BC} can be calculated using
 196 equation (3-15) (supplementary methodology S1), as stated in Rathod and Sahu (2022). The
 197 AAE for both BC and BrC can be expressed as σ , and in this study, the AAE definition by
 198 Moosmüller et al. (2011a) was used instead of the AAE specified for a wavelength pair. This
 199 value is determined by equation (32), which calculates the negative log-log slope of the
 200 absorption spectrum at wavelength λ .

201
$$AAE_{BC} = - \frac{d \ln \sigma_{BC}}{d \ln \lambda}$$

 202 _____ Eq. (3)

Formatted: Subscript

Formatted: Subscript

Formatted: Subscript

Formatted: Subscript

Formatted: Subscript

Formatted: Subscript

Formatted: Subscript

Formatted: Subscript

203 Instead of the conventional approach where AAE_{BC} is assumed to be 1, we utilized the AAE_{BC}
 204 that was observed onsite to calculate $\sigma_{BC}(\lambda)$. Equation (43-16) was employed to determine σ_{BC}
 205 (370 nm) by substituting $\sigma_{BC}(\lambda)$ at 370 nm, which was obtained using equation (23) (Wang et
 206 al., 2020), into equation (43-13) (refer to supplementary methodology S1.1, S1.2, and Figure
 207 S2 for details).

$$208 \sigma_{BrC}(370 \text{ nm}) = \sigma_{BC+BrC}(370 \text{ nm}) - \beta(370 \text{ nm})^{-AAE_{BC}(370 \text{ nm})} - AAE_{BrC} \quad \text{Eq. (4)}$$

210 To calculate $\sigma_{BrC}(\lambda)$ at 470 nm and 520 nm, we can subtract the modelled BC from
 211 the measured absorption coefficients, in a similar manner. It is worth noting that the BrC
 212 absorption coefficients are very low at wavelengths beyond 590 nm (Wang et al., 2020),
 213 according to Rathod et al. (2017) and Rathod and Sahu (2022), hence they are not taken into
 214 account (supplementary methodology S1).

215 3.2 Data Analysis

216 LULC change also has a direct impact on vehicular emissions and other anthropogenic
 217 activities. Urbanization, conceivably, can lead to increased vehicle traffic and emissions,
 218 which can contribute to air pollution and climate change. Changes in land use can also affect
 219 the amount and type of vegetation, which can influence the carbon cycle and the amount of
 220 greenhouse gases in the atmosphere. The ERA-5 reanalysis data has been used for
 221 meteorological analysis viz. wind pattern, precipitation, relative humidity, and temperature
 222 (Hersbach et al., 2020). The hourly data has been taken for the analysis and then the daily,
 223 monthly, and seasonal average has been computed for the study period over the Sikkim and
 224 surrounding states for a better understanding of the meteorological conditions influencing the
 225 BC, and BrC. The ERA5 validation with AWS data can be seen in the supplementary section
 226 (Figure S8). The total precipitation is computed as a sum of the hourly data for a day to daily
 227 total precipitation and further, it was summed for monthly cumulative total precipitation using
 228 the sum formula as

$$229 \text{ Monthly Cumulative Total Precipitation} = \sum_i^n X \quad \text{Eq. (5)}$$

230 Where, 'i' is the initial and 'n' the last date and X is the hourly total precipitation taken from
 231 ERA5. The wind circulation has been computed using the u-component and v-component of
 232 wind and the wind speed has been calculated as

$$233 \text{ Wind Speed} = \sqrt{u^2 + v^2} \quad \text{Eq. (6)}$$

Formatted: Subscript

Formatted: Subscript

Formatted: Subscript

Formatted: Subscript

Formatted: Subscript

Formatted: Subscript

234 The temperature and relative humidity averaged have been computed using [the](#) mean formula
235 as

$$236 \quad \text{Average} = \frac{\sum_i^p x}{n} \quad \text{Eq. (7)}$$

237 Where, 'i' is [the](#) initial and 'n' last date of the ~~of~~ variables such as temperature, relative
238 humidity, and wind components.

239 Let x and y be two real-valued random variables such that the correlation coefficient ~~spearman~~
240 [Spearman](#) Pearson can be calculated between the BC/BrC and meteorological parameters. The
241 Coefficient of Pearson Correlation (PCC) (Pearson, 1909; Benesty et al., 2009) as

$$242 \quad PCC = \frac{n(\sum xy) - (\sum x)(\sum y)}{\sqrt{[n \sum x^2 - (\sum x)^2][n \sum y^2 - (\sum y)^2]}} \quad \text{Eq. (8)}$$

243 Where 'n' is the population size of the variables used for the study.

244 Table 1 contains additional information about the dataset, and a more detailed methodology
245 can be found in the supplementary section (S1).

246 **4.0 Results and Discussions**

247 The anthropogenic activities in Gangtok ~~are have~~ drastically increased in [the](#) last 20 years. As
248 evident from ~~figure~~ [Figures](#) 1b, c, and d, LULC has been changed ~~since from~~ 2000 to 2020
249 over the Gangtok ~~municipal e~~ [Municipal Corporation](#) (GMC). ~~The p~~ Population change and
250 growth have also been observed ~~over in~~ the Sikkim (Table S1). LULC during [the years](#) 2000
251 and 2010 evidently shows that most of the fallow land has been built-up due to [a](#) recent change
252 in the policy of construction in Sikkim suggesting urban settlement load over Gangtok ~~is has~~
253 increased significantly. As a result, there is a significant increase in built-up areas in GMC for
254 [the last 20 years](#). The vegetation cover has also reduced ~~since from~~ 2000 to 2020 (~~F~~ [Figure](#) 1b,
255 c, and d). The rainfed water bodies are reducing from the GMC. However, due to its
256 seasonal nature, streams are lesser emerged in 2020. Which perhaps shows the precipitation
257 pattern alteration over GMC due to [the](#) highly built-up sprawl. The built-up extent has been
258 sprawling and consuming the dense vegetation regions as well. This increases the study
259 region's urge to be acknowledged so that Sikkim's future policymakers can consider the effects
260 of rising anthropogenic activities. This anthropogenic activity ~~leading leads~~ to [a](#) heavy load on
261 [the environment](#) over one of the cleanest states of India. Long-term spatiotemporal variation
262 of 2-meter air temperature justifies the LULC change and warming pattern ([Xiao-lei et al.,](#)
263 [2022](#)) over the Gangtok region ([F \[Figure\]\(#\) S1a, S1b, S1c, S1d, and S1e\). The decadal warming](#)

264 rate is varying from 0.25^o to 0.45^oC (Ffigure S1e). Thereafter, BC and BrC over the Gangtok
265 ~~has have~~ been measured to report the issue and get more attention to the scientific and local
266 community. The higher anthropogenic activity releases ~~the a~~ higher amount of emission in the
267 name of development due to ~~the~~ population load on the region (Shaddick et al., 2020) (i.e., ~~the~~
268 growth rate has been raised from 12.89 to 13.05% in recent years) (Table S14). Diurnal
269 variation of the BC, BrC, ~~BC~~ BC_{pb}, ~~BC~~ BC_{fr}, and CO₂ ~~apparently~~ show two peaks. BC, BC_{fr},
270 and CO₂ have almost similar time of peaks observed. The first peak is found during 8-10 AM.
271 And, the second peak is observed during 8-10 PM. However, BrC and BC_{pb} have the peak
272 concentration during 10-11 AM ~~and 6-8 PM~~ (Ffigure 2a), ~~suggesting the peak biomass burning~~
273 ~~time over the region~~. The ~~same for~~ meteorological conditions ~~is are~~ observed ~~as low dewpoint,~~
274 ~~low temperature, high surface pressure, low wind speed, and high relative humidity to the~~
275 ~~corresponding 8-10 AM, while the opposite is found in 8-10 PM~~ and referred to ~~figure~~ Figure
276 2b.

Formatted: Subscript
Formatted: Subscript
Formatted: Subscript
Formatted: Subscript
Formatted: Subscript

277 The daily time series of the BC, BC_{pb}, BC_{fr}, BrC, BB%, and CO₂ show the highest fluctuation
278 ~~during from~~ 20th to 30th March in both 2021 and 2022 years respectively. The maximum BC
279 (BrC) content was found in March 2022 (April-2021), at 43.5 $\mu\text{g}/\text{m}^3$ (32 $\mu\text{g}/\text{m}^3$). The lowest
280 fluctuation is observed ~~during from~~ 15th May to 15th September 2021 (Ffigure 3a). The intense
281 peaks of BC, BC_{fr} and CO₂ ~~has been were~~ observed ~~during from~~ 10th October to 15th November
282 2021 (Ffigure 3a) ~~that which~~ may be linked to the heavy tourist season of the state and
283 ~~indicating indicate towards~~ the traffic overload in the Gangtok (Sharma et al, 2022). ~~As, T~~
284 the meteorological conditions ~~are also favour favouring the~~ similar circumstances to accumulate
285 the pollutant ~~during from~~ 10th October to 15th November 2021 (Ffigure 3b). The lowest surface
286 pressure with minimum fluctuation and the highest temperature and dewpoint temperature with
287 minimum fluctuation ~~is being was~~ noticed ~~during from~~ the 15th June to 20th September 2021
288 (Ffigure 3b). ~~BrC is found to be the highest with significant variability from the 10th of January~~
289 ~~to the 30th of March, pointing to winter wood burning for livelihood, which is also supported~~
290 ~~by BC_{pb} (Table S3). BrC is found the highest with maximum fluctuation during 10th January~~
291 ~~to 30th March that is pointing towards winter wood burning for the subsistence as similar~~
292 ~~observed BC_{pb}~~. The monthly variations of BC, BC_{pb}, BC_{fr}, BrC, ~~and BB%~~ ~~is are~~ discussed in
293 ~~figure~~ Figure 4a, and the highest value of standard deviation ~~were was~~ observed during March
294 2022 for BC, BC_{fr}, and April 2021 for BC_{pb}, BrC, ~~and BB%~~. The CO₂ is observed almost
295 constant with a small value of standard deviation. The maximum concentration of the BC, BC_{fr}
296 is found in March 2022. However, BC_{pb} and BrC were measured highest in April 2021 (Table
297 S3). ~~This is probably inferring to high tourist season (i.e., vehicular emission) as well as~~

Formatted: Subscript
Formatted: Subscript

Formatted: Subscript

Formatted: Superscript
Formatted: Superscript
Formatted: Subscript

Formatted: Subscript
Formatted: Subscript
Formatted: Subscript
Formatted: Subscript
Formatted: Subscript

298 random wood burning at higher altitude regions surrounding the Gangtok. –The minimum
299 concentration of the BrC was seen in the month of August 2021 as the highest total
300 precipitation month with high wind speed, temperature ~~and~~ dewpoint temperature, and relative
301 humidity (Figure 4b, S3, and S4) (Rana et al., 2023).

302 The good correlation between BC and BC_{ff} showed that the primary source of BC is fossil fuel
303 combustion (Osborne et al, 2008; Jung et al., 2021). A significant correlation between BC_{bb}
304 and BrC indicates that biomass burning is a major contributor to BrC (Prabhu et al., 2020),
305 which is supported by the BB% and BrC (Figure 5). The ~~The good significant correlation~~
306 between BC and BC_{ff} suggested that the major contribution of the BC is fossil fuel burning
307 (Osborne et al, 2008). A strong significant correlation between BC_{bb} and BrC indicating that
308 major contributor of BrC is biomass burning that can be justified by BB% and BrC strong
309 significant positive correlation coefficient (figure 5). A good significant positive correlation
310 between CO₂ and BC/BC_{ff} suggesting suggests that fossil fuel burning is influencing one of the
311 causes the of CO₂ concentration or vis versa (Rana et al., 2023). Dewpoint temperature and CO₂
312 has ~~ve strong a significant positive positive correlation coefficient~~ suggesting ~~to~~ positive
313 radiative forcing of the CO₂ (Huang et al., 2017; Stjern et al., 2023). The SA similar has been
314 found for the temperature. BC_{bb}/BrC and temperature ~~has have a strong significant negative~~
315 correlation suggesting the negative radiative nature of the BC_{bb}/BrC (Figure S5). Moreover,
316 net thermal/solar radiation (STR/SSR) and BC/BrC have a significant positive correlation
317 (Figure 5, and S5) (Liu et al., 2020). A strong significant positive correlation between surface
318 pressure and BC/BC_{ff} (BC_{bb}/BrC) has been observed (Figure 5). Higher the surface pressure
319 ~~makes creates~~ calm conditions and a stable boundary layer, which keeps the pollutants
320 accumulated in the boundary layer (Igarashi et al., 1988; Lee et al., 1995; Bharali et al., 2019;
321 Liu et al., 2021). However, the opposite has been observed for the wind ~~that indicates~~
322 indicating the dispersion of pollutants with a strong negative correlation. The A similar has
323 been observed for the total precipitation and all the pollutants, ~~delineates delineating~~ to wet
324 scavenging of the pollutants (Yoo et al., 2014; Ohata et al., 2016; Ge et al., 2021; Wu et al.,
325 2022). The relative humidity is also showing the a similar result to the total precipitation with
326 greater values of coefficient. The negative correlation between total precipitation and surface
327 pressure ~~suggested suggests~~ that the rain falls over the region mostly occurs in a low low-
328 pressure system that is ~~causes caused~~ due to the vertical rising of an air parcel and causes ~~to~~
329 condensation and precipitation (Johnson and Hamilton, 1988; Sarkar, 2018). However, cloud
330 condensation nuclei formation and precipitation are prompted by aerosols (BC and BrC)
331 (Ohata et al., 2016; Moteki, 2023). Moreover, Thereafter, BC and BrC have crucial role in

Formatted: Subscript

Formatted: Subscript

Formatted: Subscript

Formatted: Subscript

Formatted: Subscript

Formatted: Subscript

Formatted: Subscript

332 ~~precipitation mechanism.~~ BC particles are mainly hydrophobic and less efficient as CCN
333 compared to more hydrophilic particles; they can still act as CCN under certain conditions.
334 These conditions include the size and mixing state of the particles, as well as the atmospheric
335 conditions such as relative humidity and temperature (Ohata et al., 2016; Moteki, 2023; Liu et
336 al., 2020). The conditions required for BC particles to efficiently play the role of CCN depend
337 on several factors, including their size, mixing state, and atmospheric conditions (Moteki,
338 2023; Liu et al., 2020). For example, smaller BC particles are more efficient as CCN than
339 larger ones (Moteki, 2023). The mixing state of BC particles also plays a role, as externally
340 mixed BC particles are less efficient as CCN than internally mixed ones (Liu et al., 2020).
341 Atmospheric conditions such as relative humidity and temperature also affect the efficiency of
342 BC particles as CCN (Moteki, 2023). For example, higher relative humidity and lower
343 temperatures can increase the efficiency of BC particles as CCN (Moteki, 2023). Additionally,
344 relative humidity over the study region is very high during the entire year with the favorable
345 temperature. Thereafter, BC and BrC have a crucial role in the precipitation mechanism (Zhu
346 et al., 2021; Li et al., 2023a) over the study region.

347 Total precipitation and wind circulation indicated that the study region received precipitation
348 throughout each month of the study period (i.e., most of the time in the form of rain and
349 occasionally snow). Hence the maximum is observed in August and the minimum in March
350 2022. The wind pattern illustrates the monsoon seasonal strong influence from May to
351 September 2021 (Figure 6). The wind converges in the valley and diverges from the mountain
352 for the rest of the period (figure 6). Because the strong wind and heavy rainfall indicated
353 pollution scavenging (rain out or wash out), it is significantly negatively correlated as TP vs
354 BC_{pb}; TP vs BC_{ff}; TP vs BrC (Figure 5).

355 ~~Total precipitation and wind circulation suggested that the study region is receiving~~
356 ~~precipitation in entire month of the study period (i. e., most of the time rain form and sometimes~~
357 ~~snow). As the maxima is observed during the month of August and minima during March~~
358 ~~2022. The wind pattern delineates during the May to September 2021 the monsoon seasonal~~
359 ~~strong effect (figure 6). And rest of the period the wind is converging in the valley and~~
360 ~~diverging from the mountain (figure 6). The strong wind and heavy rain fall suggested the~~
361 ~~pollutant scavenging (rain out or wash out) that is why it is significant negatively correlated.~~
362 The relative humidity and temperature follow the same pattern when the temperature gradients
363 change from January to December, resulting in a decrease in moisture content in the
364 atmosphere (Figure S6). The relative humidity and temperature patten also justify the same as
365 the temperature gradients change from January to December and moisture content reduction

Formatted: Subscript

Formatted: Subscript

366 ~~in the atmosphere (figure S6).~~ The lowest in the month of February is observed and the
367 temperature gradient ~~getting gets~~ steep from ~~the~~ November (Figure S6). The dewpoint
368 temperature contour and surface pressure shading match well suggesting that the surface
369 pressure creates the dewpoint temperature gradient and keeps it sustained and stable
370 atmospheric condition (Jung et al., 2023) (Figure S7). During the month of June, it is very
371 peculiar that the dewpoint temperature contours are wide and a very small gradient is observed
372 (Figure 7). ~~Which This is pointing points~~ toward the warm conditions during the June over
373 entire Sikkim. The cloud cover and convective precipitation over Sikkim are discussed in
374 Figure 7. Figure 7 discusses about the cloud cover and convective precipitation over the
375 Sikkim. It is clear from (figure-Figures 7a to d) that the region is not receiving ~~the~~ much
376 convective precipitation even if there is huge cloud cover, which leads to a conclusion of
377 orographic precipitation over the region (Figure 7). However, the relative humidity is very
378 high over the sampling site from the lower to upper middle level of the atmosphere during the
379 study period (Figure S3). Most of Sikkim receives convective rain from May to September,
380 which indicates that the region has strong convective activity added from the Bay of Bengal
381 during the monsoon season ~~During May to September the convective rain is receiving most~~
382 ~~part of the Sikkim approved that the region has high convective activity added from the Bay~~
383 ~~of Bengal as the monsoon season~~ (Rahman et al., 2012; Kumar et al., 2020b; Kakkar et al.,
384 2022; Biswas and Bhattacharya, 2023). Again, from October to April, the region ~~is does~~ not
385 ~~receiving receive~~ ~~the~~ convective rain even though there is strong cloud cover pointing toward
386 the orographic rainfall over the entire Sikkim (Kumar and Sharma, 2023). That's making the
387 Sikkim unique weather conditions (figure-Figures S3 and S4). The ERA5 validation with AWS
388 data can be seen in the supplementary section (Figure S8). And, ~~the~~ least concentration of BC,
389 BC_f, BC_{pb}, and BrC is observed during the monsoon months. This observation supports the
390 convective rain, as rain out scavenging, of all pollutants (Liu et al., 2020; Moteki, 2023).
391 During the monsoon season, the region experiences high convective activity, which is added
392 from the Bay of Bengal (Brooks et al., 2019; Liu et al., 2020; Moteki, 2023; Sankar et al.,
393 2023). Convective rain is an effective process for removing air pollutants from the atmosphere
394 (Liu et al., 2020; Moteki, 2023). ~~least concentration of BC, BC_f, BC_{pb} and BrC is observed~~
395 ~~during the monsoon months supporting the convective rain (i.e., rain out scavenging) of all~~
396 ~~pollutants.~~ Wet removal of BC and BrC occurs via cloud particle formation and subsequent
397 conversion to precipitation or impaction processes with hydrometeors below clouds during
398 precipitation (Liu et al., 2020; Moteki, 2023; Sankar et al., 2023). The BC and BrC have a
399 significant positive correlation with thermal and solar radiation, indicating positive radiative

Formatted: Subscript

Formatted: Subscript

400 feedback (Zhang et al., 2020; Wang et al., 2021; Li et al., 2023a). A stronger negative
401 correlation between CO₂ and surface thermal radiation (STR) and surface solar radiation (SSR)
402 would have significant implications (Figure 5). The negative correlation between CO₂ and
403 STR implies that as the concentration of CO₂ in the atmosphere increases, the amount of heat
404 radiated-radiating from the Earth's surface into space decreases (Zhang et al., 2020). This can
405 lead to an increase in the Gangtok's temperature, which can have various impacts on climate
406 and weather as well (figure-Figures S1, and 5). The negative correlation between CO₂ and SSR
407 implies that as the concentration of CO₂ in the atmosphere increases, the amount of solar
408 radiation absorbed by the Earth's surface decreases (Davis, 2017; Zhang et al., 2020; Li et al.,
409 2023b) (Figure 5). Overall, a significant negative correlation between CO₂ and STR/SSR
410 would indicate a stronger influence of greenhouse gas concentrations on the surface's radiation
411 balance (Chiodo et al., 2018) and would have important implications for climate change as
412 well as anomalous warming over the Gangtok region (Figure S1).

413 5.0 Conclusions

414 In accordance with the LULC between 2000 and 2010, Sikkim's recent changes to its
415 development regulations have resulted in the majority of fallow land being consumed by
416 construction, which suggests that Gangtok's urban settlement load has increased significantly.
417 In addition, the LULC for 2020 depicts a booming built-up region over the GMC. Since-From
418 2000 to 2020, the vegetation cover has likewise decreased. However, due to the seasonal
419 nature, streams are lesser in 2020, indicating precipitation pattern variation over GMC. The
420 areas covered in dense vegetation are also being consumed by the expanding built-up area. The
421 present study is the report of newly produced data BC and BrC for the fragile region of the
422 Himalayas and its relation with meteorological conditions. It has been observed that the
423 temperature over Gangtok is increasing as well. The peak concentration of BC/BrC has been
424 found during October 2021, and-March 2021, and 2022. The diurnal distribution of BC/BrC
425 suggests the two peaks in a day, first in-at the-8-10_AM and second in-at 9-11_PM. The
426 meteorological conditions for the same has-have been observed to be favorable to diurnal
427 variation of BC/BrC concentration. In-†The monthly variation of the BC/BrC is-delineated that
428 the peak concentration of BC, BC_{pb}, and BC_{fr}, during March 2022. However, BrC and BB%
429 have maximum concentration during April 2021. BB% and BrC as well as BB and carbon
430 dioxide have a strong significant positive correlation coefficient, which is evidence that
431 biomass burning is a substantial factor in the rise in carbon dioxide levels. In addition to this,
432 there is a strong, positive correlation between CO₂ and BC/BC_{fr}, indicating that burning fossil
433 fuels is also one of the causes of rising CO₂ levels. The net thermal radiation, net solar

Formatted: Subscript

Formatted: Subscript

Formatted: Subscript

Formatted: Subscript

Formatted: Subscript

Formatted: Subscript

Formatted: Subscript

Formatted: Subscript

Formatted: Subscript

434 radiation, and BC, BrC relationship suggested that ~~the~~ BC_r and BrC have positive radiative
435 forcing. Furthermore, the monsoon months show the lowest concentrations of BC, BC_{bb}, BC_{fr},
436 BrC, and BB%, demonstrating the convective rain (i.e., rain out scavenging) ability to remove
437 a majority of contaminants. Both the BC and BrC reveal evidence of positive radiative
438 feedback.

439 **Data Availability**

440 Data is provided in the 'supplementary section' and for further detail knowledge about it can
441 be available from the corresponding author on the adequate request.

442 Data link for the data access:

443 [https://docs.google.com/spreadsheets/d/1N4F_ft68syY6n0UIfA6nzI5o-
444 8LUWjyFfk5NpfquRyg/edit?usp=sharing](https://docs.google.com/spreadsheets/d/1N4F_ft68syY6n0UIfA6nzI5o-8LUWjyFfk5NpfquRyg/edit?usp=sharing)

445 **Conflict of Interest**

446 None conflict of interest.

447 **Authors Contribution**

448 Dr. Pramod Kumar: conceptualization, drafting, writing, figures, and editing

449 Ms. Khushboo Sharma: sampling, data analysis, and figures.

450 Ms. Ankita Malu: data analysis, figures, and editing

451 Mr. Rajeev Rajak: editing

452 Ms. Aparna Gupta: editing

453 Mr. Bidyutjyoti Baruah: editing

454 Mr. Jayant Sharma: sampling

455 Dr. Shailesh Yadav: editing, and mentoring

456 Dr. Thupstan Angchuk: editing, and mentoring

457 Dr. Rakesh Kumar Ranjan: conceptualization, data interpretation, mentoring, and editing.

458 Dr. Nishchal Wanjari: editing and mentoring.

459 Dr. Anil Kumar Misra: editing and mentoring.

460 **Acknowledgements**

461 Authors acknowledge to the Department of Science and Technology, Government of India,
462 and host department "DST's Centre of Excellence (CoE), at Department of Geology, Sikkim
463 University, DST/CCP/CoE/186/2019 (G)," for the generation of BC/BrC data. We also
464 acknowledge to free data sources used in the study as ERA5, [and](#) USGS earth explorer.

Formatted: Subscript

Formatted: Subscript

465 Authors appreciate freely available software such as R-studio, QGIS, CDO, and GrADS used
466 for the analysis and visualization. We also acknowledge [Anirud Rai, Kuldeep Dutta, Abhinav](#)
467 [Tiwari, Richard Rai, and](#) the anonymous persons who ~~m~~ so ever have helped and supported ~~for~~
468 the Black Carbon data collection.

469 **References**

- 470 [Adeeyo, R.O., Edokpayi, J.N., Volenzo, T.E., Odiyo, J.O. and Piketh, S.J., \(2022\).](#)
471 [Determinants of solid fuel use and emission risks among households: insights from Limpopo,](#)
472 [South Africa. *Toxics*, 10\(2\), p.67. <https://doi.org/10.3390/toxics10020067>](#)
- 473 Aithal, B. H., & MC, C. (2019). Assessing land surface temperature and land use change
474 through spatio-temporal analysis: a case study of select major cities of India. *Arabian Journal*
475 *of Geosciences*, 12(11), 1-16. <https://doi.org/10.1007/s12517-019-4547-1>
- 476 [Ayompe, L.M., Davis, S.J. and Egoh, B.N., \(2021\). Trends and drivers of African fossil fuel](#)
477 [CO₂ emissions 1990–2017. *Environmental Research Letters*, 15\(12\), p.124039. DOI](#)
478 [10.1088/1748-9326/abc64f](#)
- 479 Benesty, J., Chen, J., Huang, Y., and Cohen, I. (2009). Pearson correlation coefficient. In *Noise*
480 *reduction in speech processing* (pp. 1-4). Springer, Berlin, Heidelberg.
481 https://doi.org/10.1007/978-3-642-00296-0_5
- 482 Bharali, C., Nair, V. S., Chutia, L., & Babu, S. S. (2019). Modeling of the effects of wintertime
483 aerosols on boundary layer properties over the Indo Gangetic Plain. *Journal of Geophysical*
484 *Research: Atmospheres*, 124(7), 4141-4157. <https://doi.org/10.1029/2018JD029758>
- 485 Bhat, M. A., Romshoo, S. A., & Beig, G. (2022). Characteristics, source apportionment and
486 long-range transport of black carbon at a high-altitude urban centre in the Kashmir valley,
487 North-western Himalaya. *Environmental Pollution*, 305, 119295.
488 <https://doi.org/10.1016/j.envpol.2022.119295>
- 489 Bisht, D.S., Dumka, U.C., Kaskaoutis, D.G., Pipal, A.S., Srivastava, A.K., Soni, V.K., Attri,
490 S.D., Sateesh, M. and Tiwari, S., (2015). Carbonaceous aerosols and pollutants over Delhi
491 urban environment: temporal evolution, source apportionment and radiative forcing. *Science*
492 *of the Total Environment*, 521, 431-445. <https://doi.org/10.1016/j.scitotenv.2015.03.083>
- 493 [Biswas, J. and Bhattacharya, S., \(2023\). Future changes in monsoon extreme climate indices](#)
494 [over the Sikkim Himalayas and West Bengal. *Dynamics of Atmospheres and Oceans*, 101,](#)
495 [p.101346. <https://doi.org/10.1016/j.dynatmoce.2022.101346>](#)
- 496 Bond, T. C., Streets, D. G., Yarber, K. F., Nelson, S. M., Woo, J. H., & Klimont, Z. (2004). A
497 technology-based global inventory of black and organic carbon emissions from combustion.
498 *Journal of Geophysical Research: Atmospheres*, 109(D14).
499 <https://doi.org/10.1029/2003JD003697>
- 500 [Brooks, J., Liu, D., Allan, J.D., Williams, P.I., Haywood, J., Highwood, E.J., Kompalli, S.K.,](#)
501 [Babu, S.S., Satheesh, S.K., Turner, A.G. and Coe, H., \(2019\). Black carbon physical and](#)
502 [optical properties across northern India during pre-monsoon and monsoon seasons.](#)
503 [*Atmospheric Chemistry and Physics*, 19\(20\), pp.13079-13096. \[https://doi.org/10.5194/acp-19-\]\(https://doi.org/10.5194/acp-19-13079-2019\)](#)
504 [13079-2019](#)

505 [Chiodo, G., Polvani, L.M., Marsh, D.R., Stenke, A., Ball, W., Rozanov, E., Muthers, S. and](#)
506 [Tsigaridis, K., \(2018\). The response of the ozone layer to quadrupled CO2 concentrations.](#)
507 [Journal of Climate, 31\(10\), pp.3893-3907. doi: 10.1175/jcli-d-19-0086.1](#)

508 [Davis, W.J., \(2017\). The relationship between atmospheric carbon dioxide concentration and](#)
509 [global temperature for the last 425 million years. Climate, 5\(4\), p.76.](#)
510 <https://doi.org/10.3390/cli5040076>

511 [Evangelista, H., Maldonado, J., Godoi, R.H.M., Pereira, E.B., Koch, D., Tanizaki-Fonseca, K.,](#)
512 [Van Grieken, R., Sampaio, M., Setzer, A., Alencar, A. and Gonçalves, S.C. \(2007\). Sources](#)
513 [and transport of urban and biomass burning aerosol black carbon at the South–West Atlantic](#)
514 [Coast. Journal of Atmospheric Chemistry, 56\(3\), 225-238. https://doi.org/10.1007/s10874-](#)
515 [006-9052-8](#)

516 [Ge, B., Xu, D., Wild, O., Yao, X., Wang, J., Chen, X., Tan, Q., Pan, X. and Wang, Z., \(2021\).](#)
517 [Inter-annual variations of wet deposition in Beijing from 2014–2017: implications of below-](#)
518 [cloud scavenging of inorganic aerosols. Atmospheric Chemistry and Physics, 21\(12\), pp.9441-](#)
519 [9454. https://doi.org/10.5194/acp-21-9441-2021](#)

520 [Gupta, P., Singh, S. P., Jangid, A., & Kumar, R. \(2017\). Characterization of black carbon in](#)
521 [the ambient air of Agra, India: Seasonal variation and meteorological influence. Advances in](#)
522 [Atmospheric Sciences, 34\(9\), 1082-1094. https://doi.org/10.1007/s00376-017-6234-z](#)

523 [Hansen, A. D. A., & Schnell, R. C. \(2005\). The aethalometer. Magee Scientific Company,](#)
524 [Berkeley, California, USA, 7.](#)

525 [Hansen, J., Lacis, A., Rind, D., Russell, G., Stone, P., Fung, I., Ruedy, R. and Lerner, J. \(1984\).](#)
526 [Climate sensitivity: Analysis of feedback mechanisms. feedback, 1, 1-3.](#)

527 [Helin, A., Virkkula, A., Backman, J., Pirjola, L., Sippula, O., Aakko-Saksa, P., Väätäinen, S.,](#)
528 [Mylläri, F., Järvinen, A., Bloss, M. and Aurela, M. \(2021\). Variation of absorption Ångström](#)
529 [exponent in aerosols from different emission sources. Journal of Geophysical Research:](#)
530 [Atmospheres, 126\(10\), 2020JD034094. https://doi.org/10.1029/2020JD034094](#)

531 [Hersbach, H., Bell, B., Berrisford, P., Hirahara, S., Horányi, A., Muñoz-Sabater, J., Nicolas,](#)
532 [J., Peubey, C., Radu, R., Schepers, D. and Simmons, A. \(2020\). The ERA5 global reanalysis.](#)
533 [Quarterly Journal of the Royal Meteorological Society, 146\(730\), 1999-2049.](#)
534 <https://doi.org/10.1002/qj.3803>

535 [Huang, Y., Xia, Y. and Tan, X., \(2017\). On the pattern of CO2 radiative forcing and poleward](#)
536 [energy transport. Journal of Geophysical Research: Atmospheres, 122\(20\), pp.10-578.](#)
537 <https://doi.org/10.1002/2017JD027221>

538 [Igarashi, S., Sasaki, H. & Honda, M. \(1988\). Influence of pressure gradient upon boundary](#)
539 [layer stability and transition. Acta Mechanica 73, 187–198.](#)
540 <https://doi.org/10.1007/BF01177038>

541 [Johnson, R.H. and Hamilton, P.J., \(1988\). The relationship of surface pressure features to the](#)
542 [precipitation and airflow structure of an intense midlatitude squall line. Monthly Weather](#)
543 [Review, 116\(7\), pp.1444-1473. https://doi.org/10.1175/1520-](#)
544 [0493\(1988\)116<1444:TROSPF>2.0.CO;2](#)

545 [Johnson, M.A., Garland, C.R., Jagoe, K., Edwards, R., Ndemere, J., Weyant, C., Patel, A.,](#)
546 [Kithinji, J., Wasirwa, E., Nguyen, T. and Khoi, D.D., \(2019\). In-home emissions performance](#)
547 [of cookstoves in Asia and Africa. Atmosphere, 10\(5\), p.290.](#)
548 <https://doi.org/10.3390/atmos10050290>

549 [Jung, K.H., Goodwin, K.E., Perzanowski, M.S., Chillrud, S.N., Perera, F.P., Miller, R.L. and](#)
550 [Lovinsky-Desir, S., \(2021\). Personal exposure to black carbon at school and levels of](#)
551 [Fractional Exhaled nitric Oxide in New York city. Environmental Health Perspectives, 129\(9\),](#)
552 [p.097005. https://doi.org/10.1289/EHP8985](p.097005)

553 [Jung, C.H., Lee, H.M., Park, D., Yoon, Y.J., Choi, Y., Um, J., Lee, S.S., Lee, J.Y. and Kim,](#)
554 [Y.P., \(2023\). Parameterization of below-cloud scavenging for polydisperse fine mode aerosols](#)
555 [as a function of rain intensity. Journal of Environmental Sciences, 132, pp.43-55.](#)
556 <https://doi.org/10.1016/j.jes.2022.07.031>

557 Karra, K., Kontgis, C., Statman-Weil, Z., Mazzariello, J. C., Mathis, M., & Brumby, S. P.
558 (2021). Global land use/land cover with Sentinel 2 and deep learning. In 2021 IEEE
559 international geoscience and remote sensing symposium IGARSS (pp. 4704-4707). IEEE.
560 <https://doi.org/10.1109/IGARSS47720.2021.9553499>

561 Kedia, S., Ramachandran, S., Holben, B. N., & Tripathi, S. N. (2014). Quantification of aerosol
562 type, and sources of aerosols over the Indo-Gangetic Plain. Atmospheric Environment, 98,
563 607-619. <https://doi.org/10.1016/j.atmosenv.2014.09.022>

564 Kirchstetter, T. W., Novakov, T., & Hobbs, P. V. (2004). Evidence that the spectral
565 dependence of light absorption by aerosols is affected by organic carbon. Journal of
566 Geophysical Research: Atmospheres, 109(D21). <https://doi.org/10.1029/2004JD004999>

567 Kiran, V. R., Talukdar, S., Ratnam, M. V., & Jayaraman, A. (2018). Long-term observations
568 of black carbon aerosol over a rural location in southern peninsular India: Role of dynamics
569 and meteorology. Atmospheric Environment, 189, 264-274.
570 <https://doi.org/10.1016/j.atmosenv.2018.06.020>

571 [Kakkar, A., Rai, P.K., Mishra, V.N. and Singh, P., \(2022\). Decadal trend analysis of rainfall](#)
572 [patterns of past 115 years & its impact on Sikkim, India. Remote Sensing Applications: Society](#)
573 [and Environment, 26, p.100738. https://doi.org/10.1016/j.rsase.2022.100738](#)

574 Klimont, Z., Kupiainen, K., Heyes, C., Purohit, P., Cofala, J., Rafaj, P., Borcken-Kleefeld, J.
575 and Schöpp, W. (2017). Global anthropogenic emissions of particulate matter including black
576 carbon. Atmospheric Chemistry and Physics, 17(14), 8681-8723. [https://doi.org/10.5194/acp-](https://doi.org/10.5194/acp-17-8681-2017)
577 <17-8681-2017>

578 Kumar, M., Parmar, K. S., Kumar, D. B., Mhawish, A., Broday, D. M., Mall, R. K., &
579 Banerjee, T. (2018a). Long-term aerosol climatology over Indo-Gangetic Plain: Trend,
580 prediction and potential source fields. Atmospheric environment, 180, 37-50.
581 <https://doi.org/10.1016/j.atmosenv.2018.02.027>

582 Kumar, M., Raju, M. P., Singh, R. S., & Banerjee, T. (2017). Impact of drought and normal
583 monsoon scenarios on aerosol induced radiative forcing and atmospheric heating in Varanasi
584 over middle Indo-Gangetic Plain. Journal of Aerosol Science, 113, 95-107.
585 <https://doi.org/10.1016/j.jaerosci.2017.07.016>

586 Kumar, P., Patton, A. P., Durant, J. L., & Frey, H. C. (2018b). A review of factors impacting
587 exposure to PM_{2.5}, ultrafine particles and black carbon in Asian transport microenvironments.
588 Atmospheric environment, 187, 301-316. <https://doi.org/10.1016/j.atmosenv.2018.05.046>
589

590 Kumar, R. R., Soni, V. K., & Jain, M. K. (2020a). Evaluation of spatial and temporal
591 heterogeneity of black carbon aerosol mass concentration over India using three-year
592 measurements from IMD BC observation network. Science of the Total Environment, 723,
593 138060. <https://doi.org/10.1016/j.scitotenv.2020.138060>

594 [Kumar, P., Sharma, M.C., Saini, R. and Singh, G.K., \(2020b\). Climatic variability at Gangtok
595 and Tadong weather observatories in Sikkim, India, during 1961–2017. Scientific reports,
596 10\(1\), p.15177. <https://doi.org/10.1038/s41598-020-71163-y>](#)

597 [Kumar, P. and Sharma, M.C., 2023. Frontal changes in medium-sized glaciers in Sikkim, India
598 during 1988–2018: Insights for glacier-climate synthesis over the Himalaya. Iscience, 26\(10\).
599 DOI: 10.1016/j.isci.2023.107789](#)

600 [Kurokawa, J. and Ohara, T., \(2020\). Long-term historical trends in air pollutant emissions in
601 Asia: Regional Emission inventory in ASia \(REAS\) version 3. Atmospheric Chemistry and
602 Physics, 20\(21\), pp.12761-12793. <https://doi.org/10.5194/acp-20-12761-2020>](#)

603 Laskin, A., Laskin, J., & Nizkorodov, S. A. (2015). Chemistry of atmospheric brown carbon.
604 Chemical reviews, 115(10), 4335-4382. <https://doi.org/10.1021/cr5006167>

605 [Lee, T., Fisher, M., & Schwarz, W. \(1995\). Investigation of the effects of a compliant surface
606 on boundary-layer stability. Journal of Fluid Mechanics, 288, 37-58.
607 doi:10.1017/S0022112095001054](#)

608 [Li, S., Zhang, H., Wang, Z., Chen, Y. \(2023a\). Advances in the Research on Brown Carbon
609 Aerosols: Its Concentrations, Radiative Forcing, and Effects on Climate. Aerosol Air Qual.
610 Res. 23, 220336. <https://doi.org/10.4209/aaqr.220336>](#)

611

612 [Lin, J., Guo, Y., Li, J., Shao, M. and Yao, P., \(2023b\). Spatial and temporal characteristics of
613 carbon emission and sequestration of terrestrial ecosystems and their driving factors in
614 mainland China—a case study of 352 prefectural administrative districts. Frontiers in Ecology
615 and Evolution, 11, p.1169427. <https://doi.org/10.3389/fevo.2023.1169427>](#)

616 [Liu, D., He, C., Schwarz, J.P. and Wang, X., \(2020\). Lifecycle of light-absorbing carbonaceous
617 aerosols in the atmosphere. NPJ Climate and Atmospheric Science, 3\(1\), p.40.
618 <https://doi.org/10.1038/s41612-020-00145-8>](#)

619 [Liu, C., Huang, J., Tao, X., Deng, L., Fang, X., Liu, Y., Luo, L., Zhang, Z., Xiao, H.W. and
620 Xiao, H.Y., \(2021\). An observational study of the boundary-layer entrainment and impact of
621 aerosol radiative effect under aerosol-polluted conditions. Atmospheric Research, 250,
622 p.105348. <https://doi.org/10.1016/j.atmosres.2020.105348>](#)

623 Mahmood, R., Pielke Sr, R.A., Hubbard, K.G., Niyogi, D., Bonan, G., Lawrence, P., McNider,
624 R., McAlpine, C., Etter, A., Gameda, S. and Qian, B. (2010). Impacts of land use/land cover
625 change on climate and future research priorities. Bulletin of the American Meteorological
626 Society, 91(1), 37-46. <https://doi.org/10.1175/2009BAMS2769.1>

Formatted: Portuguese (Brazil)

Formatted: Portuguese (Brazil)

Field Code Changed

627 Massabò, D., Caponi, L., Bernardoni, V., Bove, M.C., Brotto, P., Calzolari, G., Cassola, F.,
628 Chiari, M., Fedi, M.E., Fermo, P. and Giannoni, M. (2015). Multi-wavelength optical
629 determination of black and brown carbon in atmospheric aerosols. *Atmospheric Environment*,
630 108,1-12. <https://doi.org/10.1016/j.atmosenv.2015.02.058>

631 Moosmüller, H., Chakrabarty, R. K., Ehlers, K. M., & Arnott, W. P. (2011a). Absorption
632 Ångström coefficient, brown carbon, and aerosols: basic concepts, bulk matter, and spherical
633 particles. *Atmospheric Chemistry and Physics*, 11(3), 1217-1225.
634 <https://doi.org/10.1021/acs.estlett.8b00118>

635 [Moteki, N., \(2023\). Climate-relevant properties of black carbon aerosols revealed by in situ
636 measurements: a review. *Progress in Earth and Planetary Science*, 10\(1\), pp.1-16.
637 <https://doi.org/10.1186/s40645-023-00544-4>](https://doi.org/10.1186/s40645-023-00544-4)

638 [Ohata, S., Moteki, N., Mori, T., Koike, M. and Kondo, Y., \(2016\). A key process controlling
639 the wet removal of aerosols: new observational evidence. *Scientific reports*, 6\(1\), p.34113.
640 <https://doi.org/10.1038/srep34113>](https://doi.org/10.1038/srep34113)

641 Osborne, S. R., Johnson, B. T., Haywood, J. M., Baran, A. J., Harrison, M. A. J., & McConnell,
642 C. L. (2008). Physical and optical properties of mineral dust aerosol during the Dust and
643 Biomass-burning Experiment. *Journal of Geophysical Research: Atmospheres*, 113(D23).
644 <https://doi.org/10.1029/2007JD009551>

645 Park, R.J., Kim, M.J., Jeong, J.I., Youn, D., & Kim, S. (2010). A contribution of brown carbon
646 aerosol to the aerosol light absorption and its radiative forcing in East Asia. *Atmospheric
647 Environment*, 44 (11), 1414-1421. <https://doi.org/10.1016/j.atmosenv.2010.01.042>

648 Pearson, K. (1909). Determination of the coefficient of correlation. *Science*, 30(757), 23-25.
649 DOI:10.1126/science.30.757.23

650 Pierrehumbert, R. T. (2014). Short-lived climate pollution. *Annual Review of Earth and
651 Planetary Sciences*, 42, 341-379. DOI: 10.1146/annurev-earth-060313-054843

652 [Prabhu, V., Soni, A., Madhwal, S., Gupta, A., Sundriyal, S., Shridhar, V., Sreekanth, V. and
653 Mahapatra, P.S., \(2020\). Black carbon and biomass burning associated high pollution episodes
654 observed at Doon valley in the foothills of the Himalayas. *Atmospheric Research*, 243,
655 p.105001. <https://doi.org/10.1016/j.atmosres.2020.105001>](https://doi.org/10.1016/j.atmosres.2020.105001)

656 [Rahman, H., Karuppaiyan, R., Senapati, P.C., Ngachan, S.V. and Kumar, A., \(2012\). An
657 analysis of past three decade weather phenomenon in the mid-hills of Sikkim and strategies
658 for mitigating possible impact of climate change on agriculture. *Climate change in Sikkim:
659 Patterns, impacts and initiatives*, pp.1-18. \[http://sikkimforest.gov.in/climate-change-in-
660 sikkim/2-chapter-An%20analysis%20of%20past%20three%20decade%20weather.pdf\]\(http://sikkimforest.gov.in/climate-change-in-sikkim/2-chapter-An%20analysis%20of%20past%20three%20decade%20weather.pdf\)](http://sikkimforest.gov.in/climate-change-in-sikkim/2-chapter-An%20analysis%20of%20past%20three%20decade%20weather.pdf)

661 Ramachandran, S., & Rupakheti, M. (2022). Trends in the types and absorption characteristics
662 of ambient aerosols over the Indo-Gangetic Plain and North China Plain in last two decades.
663 *Science of The Total Environment*, 831, 154867.
664 <https://doi.org/10.1016/j.scitotenv.2022.154867>

665 Ramachandran, S., Rupakheti, M., & Lawrence, M. G. (2020). Black carbon dominates the
666 aerosol absorption over the Indo-Gangetic Plain and the Himalayan foothills. *Environment
667 international*, 142, 105814. <https://doi.org/10.1016/j.envint.2020.105814>

668 Ramanathan, V., & Carmichael, G. (2008). Global and regional climate changes due to black
669 carbon. *Nature geoscience*, 1(4), 221-227. <https://doi.org/10.1038/ngeo156>

670 [Rana, A., Rawat, P. and Sarkar, S., \(2023\). Sources, transport pathways and radiative effects
671 of BC aerosol during 2018–2020 at a receptor site in the eastern Indo-Gangetic Plain.
672 *Atmospheric Environment*, p.119900. <https://doi.org/10.1016/j.atmosenv.2023.119900>](#)

673 Rathod, T. D., & Sahu, S. K. (2022). Measurements of optical properties of black and brown
674 carbon using multi-wavelength absorption technique at Mumbai, India. *Journal of Earth
675 System Science*, 131(1), 32. <https://doi.org/10.1007/s12040-021-01774-0>

676 Rathod, T., Sahu, S. K., Tiwari, M., Yousaf, A., Bhangare, R. C., & Pandit, G. G. (2017). Light
677 absorbing properties of brown carbon generated from pyrolytic combustion of household
678 biofuels. *Aerosol and Air Quality Research*, 17(1), 108-116.
679 <https://doi.org/10.4209/aaqr.2015.11.0639>

680 Reddy, M. S., & Venkataraman, C. (2002a). Inventory of aerosol and sulphur dioxide
681 emissions from India: I—Fossil fuel combustion. *Atmospheric Environment*, 36(4), 677-697.
682 [https://doi.org/10.1016/S1352-2310\(01\)00463-0](https://doi.org/10.1016/S1352-2310(01)00463-0)

683 Reddy, M. S., & Venkataraman, C. (2002b). Inventory of aerosol and sulphur dioxide
684 emissions from India. Part II—biomass combustion. *Atmospheric Environment*, 36(4), 699-
685 712. [https://doi.org/10.1016/S1352-2310\(01\)00464-2](https://doi.org/10.1016/S1352-2310(01)00464-2)

686 Runa, F., Islam, M., Jeba, F., & Salam, A. (2022). Light absorption properties of brown carbon
687 from biomass burning emissions. *Environmental Science and Pollution Research*, 29(14),
688 21012-21022. <https://doi.org/10.1007/s11356-021-17220-z>

689 [Sankar, T.K., Ambade, B., Mahato, D.K., Kumar, A. and Jangde, R., \(2023\). Anthropogenic
690 fine aerosol and black carbon distribution over urban environment. *Journal of Umm Al-Qura
691 University for Applied Sciences*, pp.1-10. <https://doi.org/10.1007/s43994-023-00055-4>](#)

692 [Sarkar, A., \(2018\). A generalized relationship between atmospheric pressure and precipitation
693 associated with a passing weather system. *MAUSAM*, 69\(1\), pp.133-140. DOI:
694 \[10.54302/mausam.v69i1.242\]\(https://doi.org/10.54302/mausam.v69i1.242\)](#)

695 Sharma, K., Ranjan, R.K., Lohar, S., Sharma, J., Rajak, R., Gupta, A., Prakash, A. and Pandey,
696 A.K. (2022). Black Carbon Concentration during Spring Season at High Altitude Urban Center
697 in Eastern Himalayan Region of India. *Asian Journal of Atmospheric Environment (AJAE)*,
698 16(1). <https://doi.org/10.5572/ajae.2021.149>

699 Shindell, D., Kuylenstierna, J.C., Vignati, E., van Dingenen, R., Amann, M., Klimont, Z.,
700 Anenberg, S.C., Muller, N., Janssens-Maenhout, G., Raes, F. and Schwartz, J. (2012).
701 Simultaneously mitigating near-term climate change and improving human health and food
702 security. *Science*, 335(6065), 183-189. DOI: [10.1126/science.1210026](https://doi.org/10.1126/science.1210026)

703 [Shaddick, G., Thomas, M.L., Mudu, P., Ruggeri, G. and Gumy, S., \(2020\). Half the world's
704 population are exposed to increasing air pollution. *NPJ Climate and Atmospheric Science*,
705 \[3\\(1\\), p.23. https://doi.org/10.1038/s41612-020-0124-2\]\(https://doi.org/10.1038/s41612-020-0124-2\)](#)

706 Shukla, K. K., Sarangi, C., Attada, R., & Kumar, P. (2022). Characteristic dissimilarities
707 during high aerosol loading days between western and eastern Indo-Gangetic Plain.
708 *Atmospheric Environment*, 269, 118837. <https://doi.org/10.1016/j.atmosenv.2021.118837>

709 Sloss, L. (2012). Black carbon emissions in India. CCC/209. IEA Clean Coal Centre, London,
710 38.

711 Stevens, B., & Feingold, G. (2009). Untangling aerosol effects on clouds and precipitation in
712 a buffered system. *Nature*, 461(7264), 607-613. <https://doi.org/10.1038/nature08281>

713 [Stjern, C.W., Forster, P.M., Jia, H., Jouan, C., Kasoar, M.R., Myhre, G., Olivié, D., Quaas, J.,
714 Samset, B.H., Sand, M. and Takemura, T., \(2023\). The Time Scales of Climate Responses to
715 Carbon Dioxide and Aerosols. *Journal of Climate*, 36\(11\), pp.3537-3551.
716 <https://doi.org/10.1175/JCLI-D-22-0513.1>](#)

717 [Sun, Y., Hao, Q., Cui, C., Shan, Y., Zhao, W., Wang, D., Zhang, Z. and Guan, D., \(2022\).
718 Emission accounting and drivers in East African countries. *Applied Energy*, 312, p.118805.
719 <https://doi.org/10.1016/j.apenergy.2022.118805>](#)

720 Takemura, T., & Suzuki, K. (2019). Weak global warming mitigation by reducing black carbon
721 emissions. *Scientific reports*, 9(1), 1-6. <https://doi.org/10.1038/s41598-019-41181-6>

722 Venkataraman, C., Habib, G., Kadamba, D., Shrivastava, M., Leon, J.F., Crouzille, B.,
723 Boucher, O. and Streets, D.G. (2006). Emissions from open biomass burning in India:
724 Integrating the inventory approach with high-resolution Moderate Resolution Imaging
725 Spectroradiometer (MODIS) active-fire and land cover data. *Global biogeochemical cycles*,
726 20(2). <https://doi.org/10.1029/2005GB002547>

727 Watham, T., Padalia, H., Srinet, R., Nandy, S., Verma, P. A., & Chauhan, P. (2021). Seasonal
728 dynamics and impact factors of atmospheric CO₂ concentration over subtropical forest
729 canopies: observation from eddy covariance tower and OCO-2 satellite in Northwest
730 Himalaya, India. *Environmental Monitoring and Assessment*, 193(2), 1-15.
731 <https://doi.org/10.1007/s10661-021-08896-4>

732 [Wang, Q., Liu, H., Ye, J., Tian, J., Zhang, T., Zhang, Y., Liu, S. and Cao, J., \(2020\). Estimating
733 Absorption Ångström Exponent of Black Carbon Aerosol by Coupling Multiwavelength
734 Absorption with Chemical Composition. *Environmental Science & Technology Letters*, 8\(2\),
735 pp.121-127. <https://doi.org/10.1021/acs.estlett.0c00829>](#)

736 [Wang, L., Jin, W., Sun, J., Zhi, G., Li, Z., Zhang, Y., Guo, S., He, J. and Zhao, C., \(2021\).
737 Seasonal features of brown carbon in northern China: Implications for BrC emission control.
738 *Atmospheric Research*, 257, p.105610. <https://doi.org/10.1016/j.atmosres.2021.105610>](#)

739 [Wu, Y., Wang, Y., Zhou, Y., Liu, X., Tang, Y., Wang, Y., Zhang, R. and Li, Z., \(2022\). The
740 wet scavenging of air pollutants through artificial precipitation enhancement: A case study in
741 the Yangtze River Delta. *Frontiers in Environmental Science*, 10, p.1027902.
742 <https://doi.org/10.3389/fenvs.2022.1027902>](#)

743 [Xiao-lei, C. H. U., L. U. Zhong, W. E. I. Dan, and L. E. I. Guo-ping., \(2022\). Effects of land
744 use/cover change on temporal and spatial variability of precipitation and temperature in the
745 Songnen Plain of China. *Journal of Integrative Agriculture* 21, no. 1: 235. doi: 10.1016/S2095-
746 3119\(20\)63495-5](#)

747 Yasunari, T., Bonasoni, P., Laj, P., Fujita, K., Vuillermoz, E., Marinoni, A., Cristofanelli, P.,
748 Duchi, R., Tartari, G. and Lau, K.M. (2010). Estimated impact of black carbon deposition
749 during pre-monsoon season from Nepal Climate Observatory–Pyramid data and snow albedo

Field Code Changed

750 changes over Himalayan glaciers. *Atmospheric Chemistry and Physics*, 10(14), 6603-6615.
751 <https://doi.org/10.5194/acp-10-6603-2010>

752 [Yoo, J.M., Lee, Y.R., Kim, D., Jeong, M.J., Stockwell, W.R., Kundu, P.K., Oh, S.M., Shin,](#)
753 [D.B. and Lee, S.J., \(2014\). New indices for wet scavenging of air pollutants \(O3, CO, NO2,](#)
754 [SO2, and PM10\) by summertime rain. *Atmospheric Environment*, 82, pp.226-237.](#)
755 <https://doi.org/10.1016/j.atmosenv.2013.10.022>

756 Yue, S., Zhu, J., Chen, S., Xie, Q., Li, W., Li, L., Ren, H., Su, S., Li, P., Ma, H. and Fan, Y.
757 (2022). Brown carbon from biomass burning imposes strong circum-Arctic warming. *One*
758 *Earth*, 5(3), 293-304. <https://doi.org/10.1016/j.oneear.2022.02.006>

759 Zhang, R., Jing, J., Tao, J., Hsu, S.-C., Wang, G., Cao, J., Lee, C. S. L., Zhu, L., Chen, Z.,
760 Zhao, Y., and Shen, Z. (2013). Chemical characterization and source apportionment of PM2.5
761 in Beijing: seasonal perspective, *Atmos. Chem. Phys.*, 13, 7053–7074,
762 <https://doi.org/10.5194/acp-13-7053-2013>

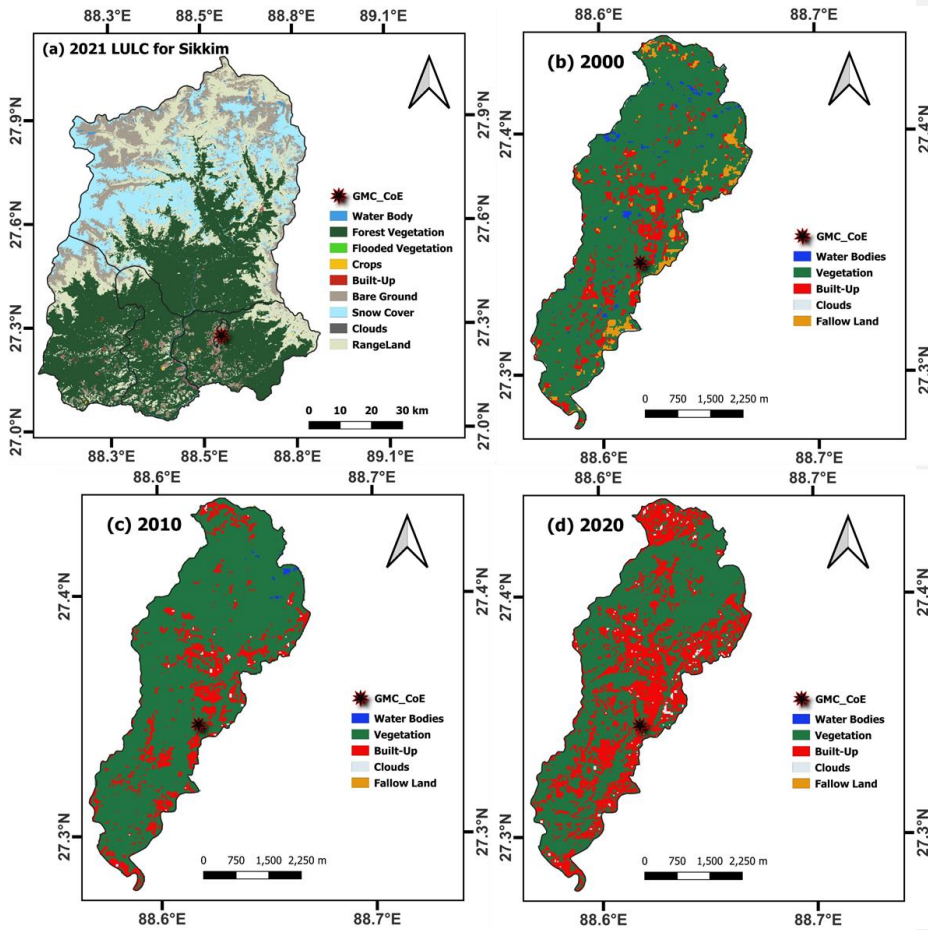
763 [Zhang, A., Wang, Y., Zhang, Y., Weber, R.J., Song, Y., Ke, Z. and Zou, Y., \(2020\). Modeling](#)
764 [the global radiative effect of brown carbon: a potentially larger heating source in the tropical](#)
765 [free troposphere than black carbon. *Atmospheric Chemistry and Physics*, 20\(4\), pp.1901-1920.](#)
766 <https://doi.org/10.5194/acp-20-1901-2020>

767 [Zhu, C.S., Ou, Y., Huang, H., Chen, J., Dai, W.T., Huang, R.J. and Cao, J.J., \(2021\). Black](#)
768 [carbon and secondary brown carbon, the dominant light absorption and direct radiative forcing](#)
769 [contributors of the atmospheric aerosols over the Tibetan Plateau. *Geophysical research letters*,](#)
770 [48\(11\), p.e2021GL092524. https://doi.org/10.1029/2021GL092524](#)

771

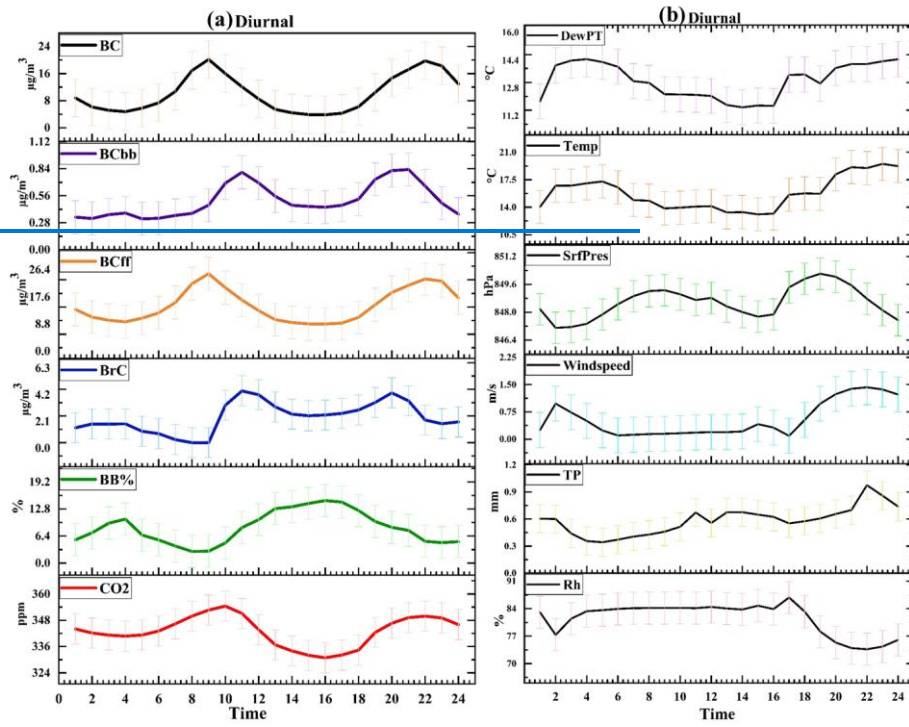
772

List of Figures

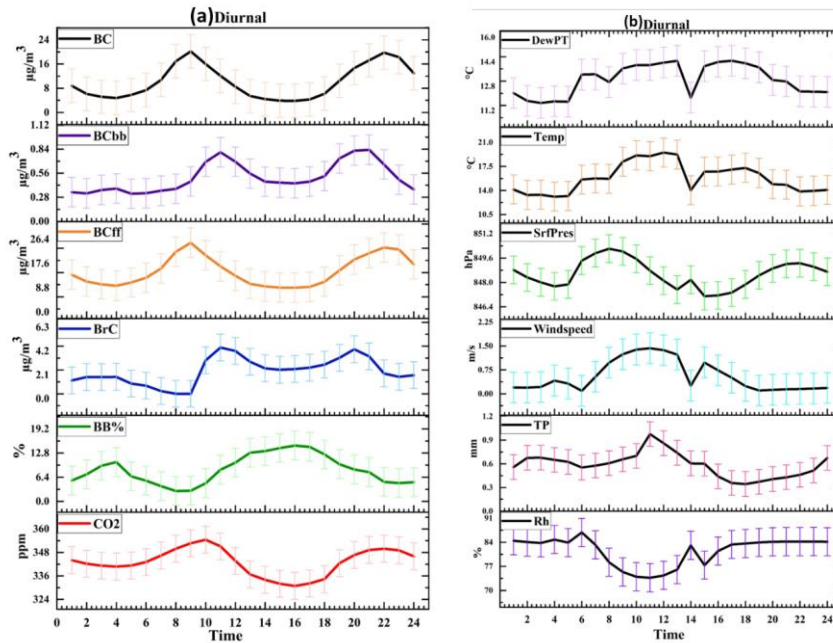


773

774 Figure 1. The study location and land use land cover for 2000, 2010, 2020, and 2021 for
775 December over Gangtok and Sikkim region using [landsatLandsat-5](#), [landsatLandsat-8](#), and
776 [Ssentinel-2](#) data sets.



777
 778
 779
 780
 781
 782
 783



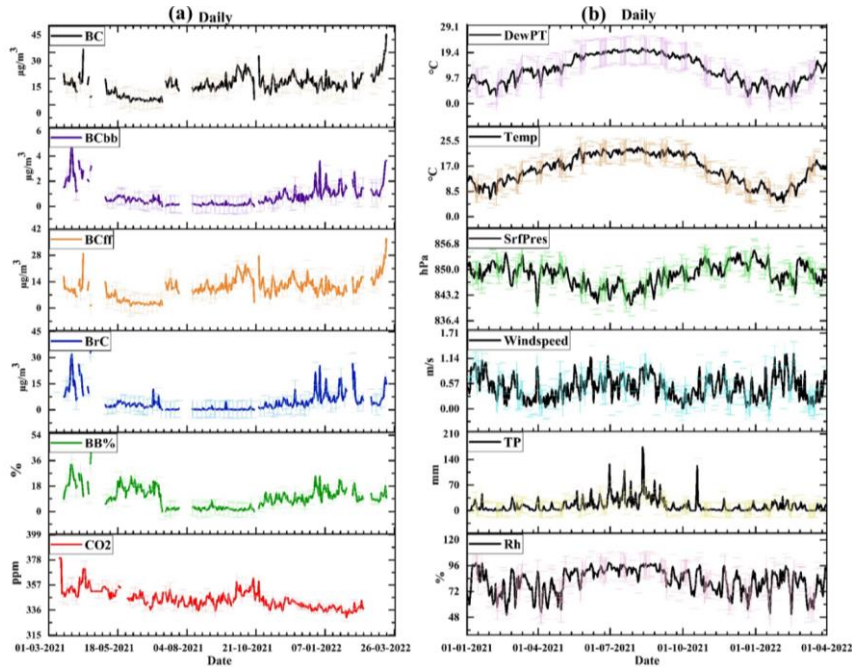
786 Figure 2. (a) The hourly observation of Black Carbon, Black Carbon through biomass burning,
 787 Black Carbon through fossil fuel, Brown Carbon, Biomass Burning percentage and Carbon
 788 Dioxide (BC, BC_{bb}, BC_{ff}, BrC, BB%, and CO₂, respectively) (The corresponding unit for BC,
 789 BC_{bb}, BC_{ff}, BrC: $\mu\text{g}/\text{m}^3$; BB%: % and CO₂: ppm) for 16th March 2021 to 10th March 2022 over
 790 study location (lat:27.32; lon:88.61). The light colour shading refers to $\pm\sigma$ standard deviation
 791 for each variable. (b) Same as figure-Figure 2a, but for meteorological parameters such as
 792 dewpoint temperature (DewPT), temperature (Temp), surface pressure (SrfPres), windspeed,
 793 total precipitation (TP), and relative humidity (Rh) during from 16th March 2021 to 10th March
 794 2022.

Formatted: Subscript

Formatted: Subscript

Formatted: Subscript

Formatted: Subscript

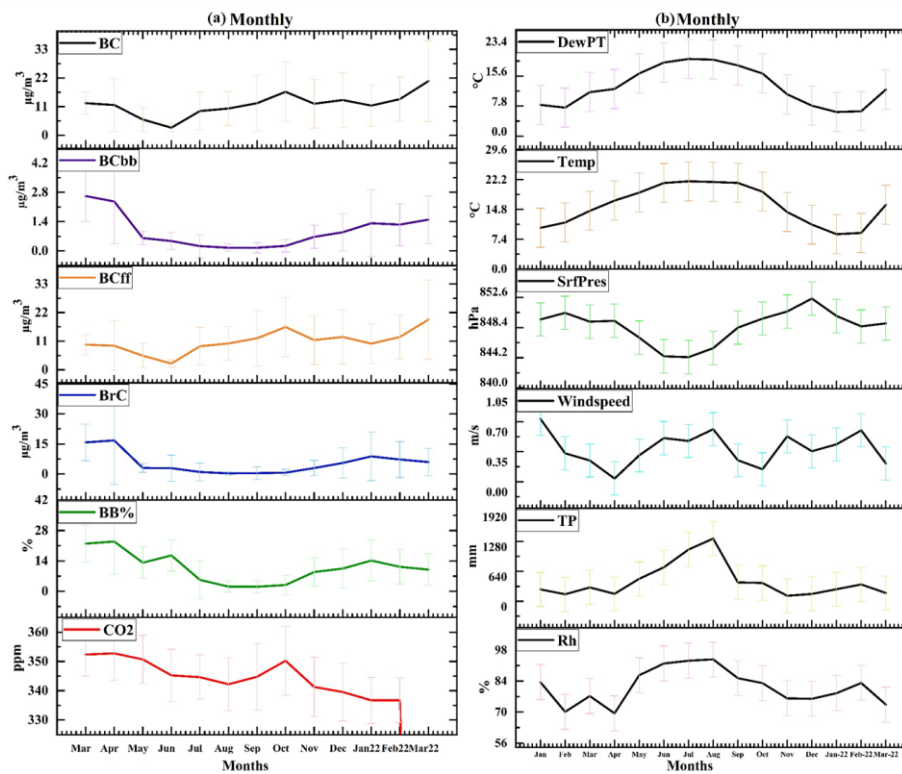


796

797 Figure 3. (a) The daily mean of Black Carbon, Black Carbon through biomass burning, Black
 798 Carbon through fossil fuel, Brown Carbon, Biomass Burning percentage and Carbon Dioxide
 799 (BC, BC_{bb}, BC_{ff}, BrC, BB%, and CO₂, respectively) (The corresponding unit for BC, BC_{bb},
 800 BC_{ff}, BrC: $\mu\text{g}/\text{m}^3$; BB%: % and CO₂: ppm) for 16th March 2021 to 10th March 2022 over study
 801 location (lat:27.32; lon:88.61). The light colour shading refers to $\pm\sigma$ standard deviation for
 802 each variable. (b) same as figure-Figure 3a, but for meteorological parameters such as dewpoint
 803 temperature (DewPT), temperature (Temp), surface pressure (SrfPres), Windspeed, total
 804 precipitation (TP), and relative humidity (Rh) during from 1st January 2021 to 31st March 2022.

805

Formatted: Subscript
 Formatted: Subscript
 Formatted: Subscript
 Formatted: Subscript

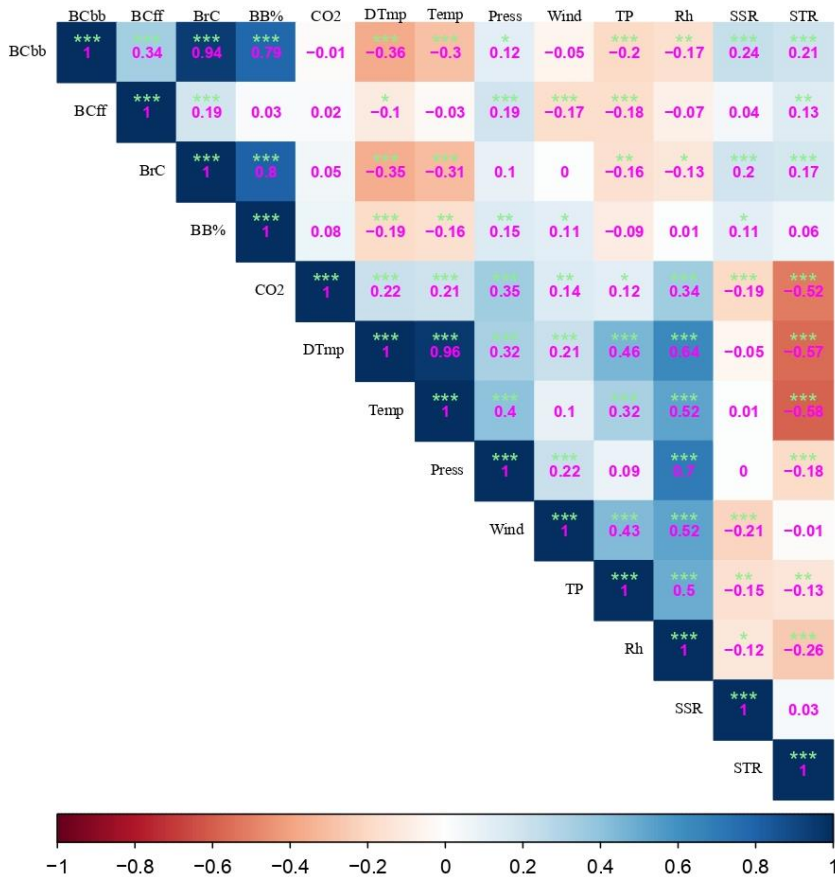


806

807 Figure 4. (a) The monthly mean of Black Carbon, Black Carbon through biomass burning,
 808 Black Carbon through fossil fuel, Brown Carbon, Biomass Burning percentage and Carbon
 809 Dioxide (BC, BC_{bb}, BC_{ff}, BrC, BB%, and CO₂, respectively) (The corresponding unit for BC,
 810 BC_{bb}, BC_{ff}, BrC: $\mu\text{g}/\text{m}^3$; BB%: % and CO₂: ppm) for 16th March 2021 to 10th March 2022 over
 811 study location (lat:27.32; lon:88.61). The error bar shows $\pm\sigma$ standard deviation for each
 812 variable. (b) Same as [figure Figure 4a](#), but for meteorological parameters [such](#) as dewpoint
 813 temperature (DewPT), temperature (Temp), surface pressure (SrfPres), windspeed, total
 814 precipitation (TP), and relative humidity (Rh) during January 2021 to March 2022.

815

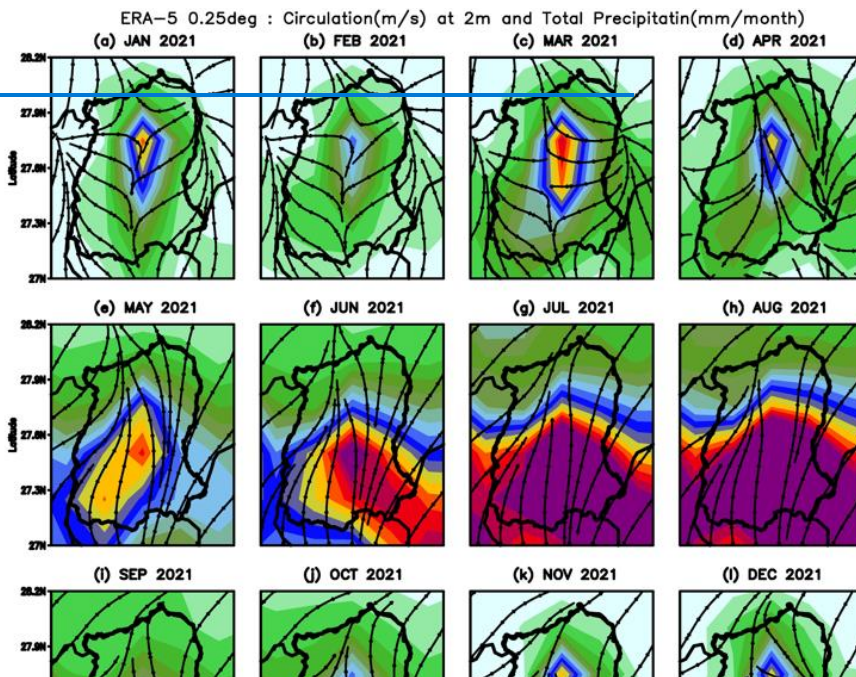
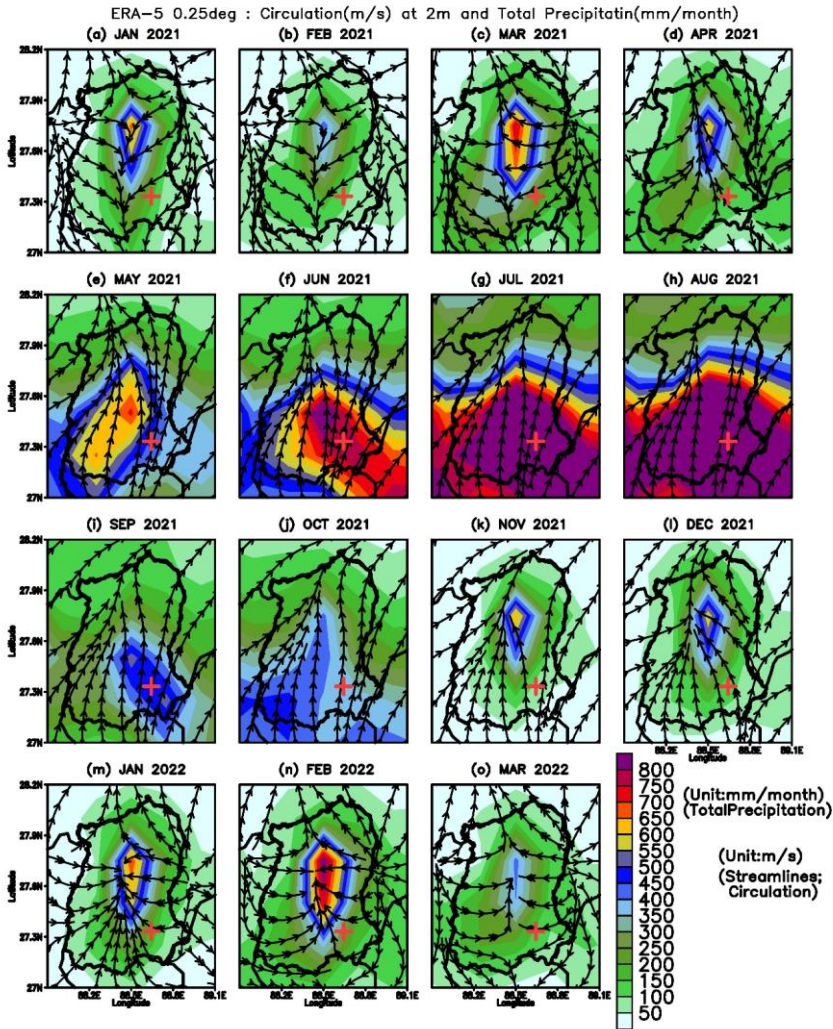
- Formatted: Subscript
- Formatted: Subscript
- Formatted: Subscript
- Formatted: Subscript
- Formatted: Subscript
- Formatted: Subscript



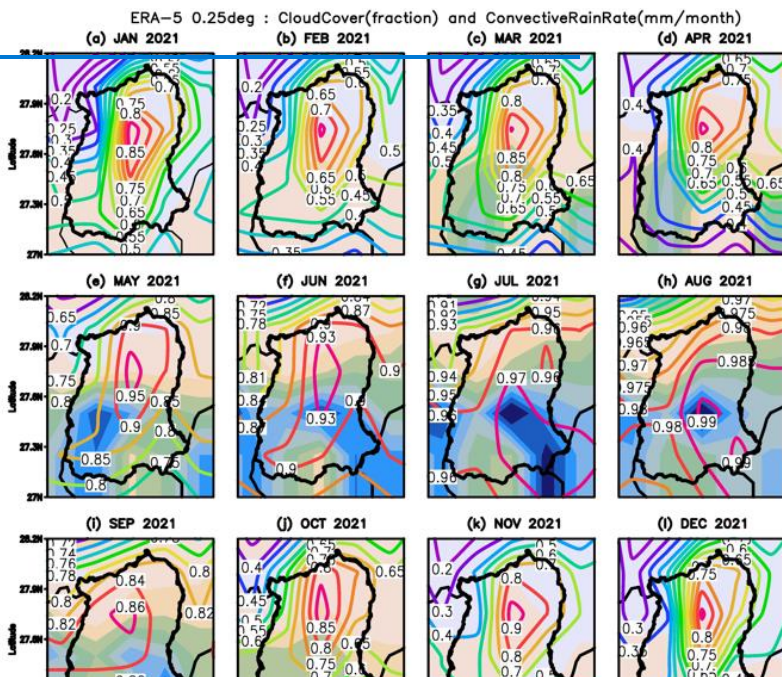
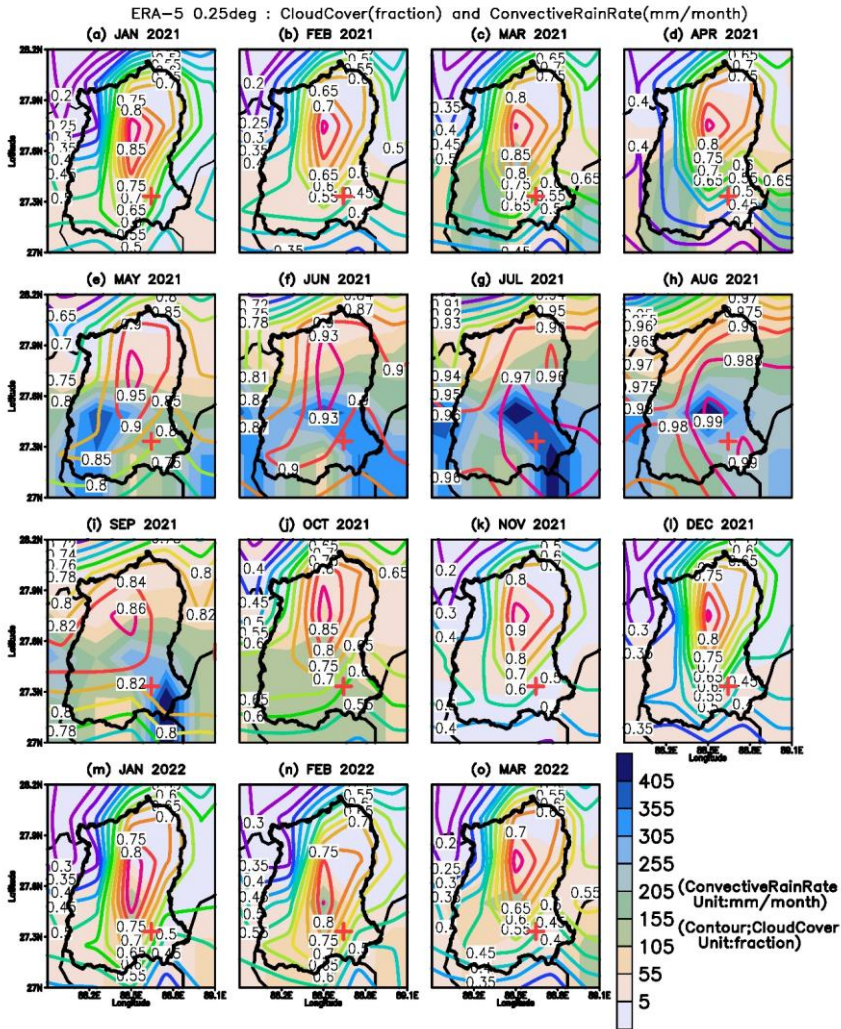
816
817
818
819
820
821
822
823

Figure 5. Correlation among BC, BC_{bb}, BC_{ff}, BrC, BB%, CO₂ and, dewpoint temperature (DTmp), temperature (Temp), surface pressure (Press), Wind, total precipitation (TP), Relative humidity (Rh), net solar radiation (SSR), and net thermal radiation (STR). The (***) shows 99% significance, (**) shows 95% significance, (*) 90% significance, and () shows no significance. The correlation coefficient values (-0.3 to -0.49) or (0.3 to 0.49) are considered as 'a good correlation', and values ≤ (-0.5) or ≥ (0.5) are considered as 'a strong correlation'.

Formatted: Subscript
Formatted: Subscript



825 Figure 6. Monthly total precipitation (cumulative) and wind circulation pattern during January
826 2021 to March 2022. The Shading shows precipitation patterns, and [the](#) streamline shows wind
827 circulation. [The \(+\) mark is a representation of the sampling location.](#)
828



830 Figure 7. Monthly convective rain and total cloud cover during January 2021 to March 2022.
831 The shading shows [a](#) convective rain pattern, and [the](#) contour shows [a](#) total cloud cover
832 fraction. [The \(+\) mark is a representation of the sampling location.](#)
833

834

List of Tables

835 Table 1. The details of datasets used for the present study.

836

Variables	Data sets	Years (Span)	Resolution		Source	Reference
			Temporal	Horizontal		
Black and Brown Carbon	Observation and analysis, data generated using Aethalometer AE33	March 2021- March 2022	Weekly	Point Location (Gangtok)	Original data generated	Present Study
Total precipitation	ERA5 (ECMWF)	2021 to 2022	Hourly	0.25° * 0.25°	ECMWF https://cds.climate.copernicus.eu/cdsapp#!/dataset/reanalysis-era5-single-levels?tab=form	Hersbach et al., 2020
Relative humidity						
Temperature (2 meter)						
Wind (surface wind)						
Surface pressure						
Dewpoint temperature						
Net solar, and thermal radiation downward						
LULC	LandSat-5, LandSat-8 and earth explorer USGS	December 2000, December 2010, December 2020	2000, 2010, 2020	30m, 30m	earth explorer USGS. https://earthexplorer.usgs.gov/	earth explorer USGS.
LULC	Sentinel-2 Esri Inc.	December 2021	2021	10 m	Esri Inc. https://www.arcgis.com/home/item.html?id=d3da5dd386d140cf93fc9ecbf8da5e31	Karra et al., 2021

Formatted: Centered

Formatted Table

Formatted: Centered

Formatted: Centered

Formatted: Centered

Formatted: Centered

Formatted: Centered

Formatted: Centered

Formatted: Centered

Formatted: Centered

Field Code Changed

Formatted: Centered

837